

Retinal Vessel Segmentation based on Possibilistic Fuzzy c-means Clustering Optimised with Cuckoo Search

Eid Emary^{*§}, Hossam M. Zawbaa^{†‡§}, Aboul Ella Hassanien^{*§}, Gerald Schaefer[¶] and Ahmad Taher Azar^{||}

^{*} Faculty of Computers and Information, Cairo University, Egypt

[†] Faculty of Mathematics and Computer Science, Babes-Bolyai University, Romania

[‡] Faculty of Computers and Information, BeniSuef University, Egypt

[§] Scientific Research Group in Egypt, <http://www.egyptscience.net>

[¶] Department of Computer Science, Loughborough University, Loughborough, U.K.

^{||} Faculty of Computers and Information, Benha University, Egypt

Abstract—Automated analysis of retinal vessels is essential for the diagnosis of a wide range of eye diseases and plays an important role in automatic retinal disease screening systems. In this paper, we present an approach to automatic vessel segmentation in retinal images that utilises possibilistic fuzzy c-means (PFCM) clustering to overcome the problems of the conventional fuzzy c-means objective function. In order to obtain optimised clustering results using PFCM, a cuckoo search method is used. The cuckoo search algorithm, which is based on the brood parasitic behaviour of some cuckoo species in combination with the Levy flight behaviour of some birds and fruit flies, is applied to drive the optimisation of the fuzzy clustering. The performance of our algorithm is analysed on two benchmark databases, the DRIVE and STARE datasets, and encouraging segmentation performance is observed.

I. INTRODUCTION

Automated segmentation of retinal vessels is typically the first step in the development of any computer-aided diagnosis system for ophthalmic disorders [1] which help ophthalmologists to screen larger populations for vessel abnormalities caused by multiple diseases such as obesity [2], hypertension [3], glaucoma [4] or diabetic retinopathy [5]. Vessel segmentation is further necessary for evaluation of retinopathy of prematurity [6], vessel diameter measurement [7], fovea region detection [8], arteriolar narrowing [9] and computer assisted laser surgery [10].

Automated retinal vessels segmentation is also at the core in development of retina-based authentication systems. Using retinal images taken from individuals, retina-based authentication is employed in environments such as nuclear research centers and facilities, and weapon factories, where extremely high security measures are needed [11]. Furthermore, automated registration of two retinal images for diagnosis or other purposes rely mainly on extracted vessel configurations [12].

The automated segmentation of vessels in retinal images can be seen as a classification problem where each pixel is classified as vessel-like or background. Several challenges make automated retinal vessel segmentation difficult [13]:

- Various structures appear in retinal images, including the optic disc, fovea, exudates and pigment epithelium changes which can disrupt vessel segmentation.

- The vessel intensity contrast is weak and varies.
- Vessels have variant bifurcations.
- Vessels have a wide range of widths.
- Small vessels are especially affected by image noise.
- Narrow vessels with various local surroundings may appear as elongated and disjoint spots and are hence difficult to identify.

In this paper, we propose a novel algorithm for automated segmentation of retinal vessels based on possibilistic fuzzy c-means (PFCM) clustering optimised by a cuckoo search technique. Experimental evaluation on the DRIVE [14] and STARE [25] datasets shows encouraging performance.

II. RELATED WORK

Automatic segmentation methods for retinal blood vessels can be categorised into supervised and unsupervised approaches. Supervised methods depend on classification into vessel and background pixels using a classifier previously trained on (manually) labelled samples. They hence require accurate ground truth data which is difficult to obtain, also as one can observe differences between manual segmentations of different ophthalmologists. On the other hand, training allows these methods to provide better performance compared to unsupervised methods, especially for images not containing pathologies.

Many methods for retinal vessel segmentation have been reported, so here we mention only a select few. Staal *et al.* [14] used a kNN classifier with a 27-dimensional feature vector based on ridge information. Their method depends on extracting ridges in the image, forming line elements from these ridges, assigning each pixel to the nearest line to partition the image into patches and computing feature vectors for each pixel based on its line and patch attributes.

Fraz *et al.* [16] used a 9-dimensional feature vector consisting of the inverted gray-level of the green colour channel, the sum of gradient orientation maps at three scales, the sum of tophat transform responses in eight directions using linear structure element, the two maximum responses of two orthogonal line detectors rotated in twelve angles and the four maximum responses of a Gabor filter rotated at ten angles

and four scales. They used an ensemble classifier from two-hundred bagged and boosted decision trees.

Marin *et al.* [15] employed 7-dimensional feature vectors comprising five features encoding gray-level variations between the pixel and its surroundings and two features based on Hu moment invariants, and trained a neural network for classification.

Unsupervised methods can be grouped into those based on mathematical morphology, vessel tracking, matched filters and bio-inspired algorithms. Mathematical morphology algorithms utilise the fact that retinal vessels have morphology of connected piecewise linear segments. Here, the top-hat transformation is widely used for blood vessel segmentation, since it estimates the background of the image using a morphological opening operation and the retinal vessels are thus enhanced when subtracting this estimated background from the original image. The advantages of mathematical morphology are the speed and noise resistance but its drawback is that it does not exploit the known shape of the retinal vessel crosssection.

Fraz *et al.* [18] extracted the centerlines of retinal vessels using a first-order derivative of Gaussian filter rotated at four orientations to detect retinal vessels in all directions. Then, the shape and orientation maps of retinal vessels are obtained by applying a morphological top-hat transform with a linear structuring element at eight directions to emphasise vessels at all possible orientations, followed by a morphological bit plane slicing of the gray-level image. The final vessel tree is reconstructed using the detected centrelines and maps of shape and orientation.

Miri and Mahloojifar [17] use the fast discrete curvelet transform for contrast enhancement and a multi-structure morphological transformation for detection of retinal vessels edges. False positive detections are pruned by morphological opening and reconstruction and by length filtering.

Illumination variation in background and presence of pathologies can lead to false positives resulting from matched filters. Zhang *et al.* [20] therefore extended matched filters by using two kernels, one based on a Gaussian and another based on the first derivative of a Gaussian to filter out false positive detections as non-vessel edges which have high responses to both kernels, while vessels have high responses only for the basic Gaussian-profiled matched filter.

Delibasis *et al.* [19] initialised the seed pixels for vessel tracking using a multiscale vesselness filter and pick a random non-zero pixel as a seed. They used a parametric model that exploits the geometric properties of retinal vessel composed of a “strip” and defined a measure of match (MoM) which quantifies the similarity between the model and the given image. Vessel tracking is performed by identifying the best matching strip of the vessel using the seed point, strip orientation, strip width and the MoM. The method actively seeks vessel bifurcation without user intervention.

III. PROPOSED ALGORITHM

A. Fuzzy *c*-means

The fuzzy *c*-means (FCM) algorithm partitions a collection of n data points into c fuzzy clusters with $c < n$, and simultaneously seeks the best possible locations of these clusters.

The method uses distance concepts in n -dimensional Euclidean space to determine the closeness of data points by assigning them to various clusters or categories.

The partitioned clusters are typically defined by a membership matrix of order $(c \times n)$ with elements U_{ik} . U_{ik} specifies the degree of membership of the k -th data point in the i -th cluster and takes on values in the interval $[0; 1]$. The sum of all memberships of any data point to all cluster centers is 1; i.e. $\sum_{i=1}^c \mu_{ik} = 1$.

The objective function for FCM is

$$\min J(M, v_1, v_2, \dots, v_c) = \sum_{i=1}^c \sum_{k=1}^n (\mu_{ik})^q (d_{ik})^2, \quad (1)$$

where q is a weighting exponent parameter that controls the extent of membership sharing between fuzzy clusters.

The following are the two necessary conditions for J to reach a minimum:

$$v_i = \frac{\sum_{k=1}^n (\mu_{ik})^q \cdot x_k}{\sum_{k=1}^n (\mu_{ik})^q}, \quad (2)$$

and

$$\mu_{ik} = \left[\sum_{j=1}^c \left(\frac{d_{ik}}{d_{jk}} \right)^{\frac{2}{q-1}} \right]^{-1}, \quad (3)$$

where x_k is the k -th data point (an m -dimensional vector) with $k = 1, 2, \dots, n$, v_i is the center of the i -th fuzzy cluster with $i = 1, 2, \dots, c$, and $d_{ik} = \|x_k - v_i\| = \left[\sum_{j=1}^m (x_{kj} - v_{ij})^2 \right]^{\frac{1}{2}}$.

B. Possibilistic *c*-means

FCM assigns memberships to objects which are inversely related to the relative distance of the point prototypes that are cluster centers in the FCM model. If a data point has equal distances to two or more clusters, then the membership to these clusters will be the same apart from the distance between the cluster centers. In this case, a better membership value should be very low or zero. To overcome this problem, [22] proposes a new clustering model, possibilistic *c*-means (PCM), which relaxes the column sum constraint equal to one, so that the sum of each column satisfies the looser constraint. In other words, each element of the i -th column can take on any value between 0 and 1. They suggested that in this case the value should be interpreted as the typicality relative to the cluster, rather than its membership to the cluster.

The objective function here is

$$\min J(T, V; X, \gamma) = \sum_{i=1}^c \sum_{k=1}^n (d_{ik})_A^2 + \sum_{i=1}^c \gamma_i \sum_{k=1}^n (1 - t_{ik})^q, \quad (4)$$

with

$$t_{ik} = \frac{1}{1 + \left(\frac{D_{ikA}^2}{\gamma_i} \right)^{\frac{1}{m-1}}}, \quad (5)$$

where $\gamma > 0$, q is weighting exponent parameter that controls the extent of membership sharing between possibilistic clusters. The larger the value of q , the more typical the membership assignments of the clusters.

The following are the two necessary conditions for J to reach a minimum:

$$v_i = \frac{\sum_{k=1}^n (t_{ik})^q \cdot x_k}{\sum_{k=1}^n (t_{ik})^q}, \quad (6)$$

and

$$t_{ik} = \frac{1}{1 + \left(\frac{D_{iKA}^2}{\gamma_i}\right)^{\frac{1}{m-1}}}. \quad (7)$$

C. Possibilistic fuzzy c-means

[21] proposes a new model to clustering that satisfies both the constraints of fuzzy c-means and possibilistic c-means. The resulting possibilistic fuzzy c-means (PFCM) clustering is characterised as

$$\min J(U, T, V; X, \gamma) = \sum_{i=1}^c \sum_{k=1}^n (a\mu_{ik}^m + b t_{ik}^n) (d_{ik})_A^2 + \sum_{i=1}^c \gamma_i \sum_{k=1}^n (1 - t_{ik})^\eta, \quad (8)$$

where $\eta > 1$.

The following are the two necessary conditions for J to reach a minimum:

$$v_i = \frac{\sum_{k=1}^n (t_{ik})^q \cdot x_k}{\sum_{k=1}^n (t_{ik})^q}, \quad (9)$$

and

$$\mu_{ik} = \left[\sum_{j=1}^c \left(\frac{d_{ik}}{d_{jk}} \right)^{\frac{2}{q-1}} \right]^{-1}. \quad (10)$$

D. Cuckoo search optimisation

Cuckoo search (CS) is a heuristic search algorithm, proposed in [23], and is inspired by the reproduction strategy of cuckoos. Cuckoos lay their eggs in the nests of other host birds, which may be of different species. The host bird may discover that an egg is not its own and either destroy the egg or abandon the nest to another. To apply this as an optimisation tool, Yang and Deb used three rules:

- Each cuckoo lays one egg, which represents a set of solution co-ordinates, at a time and drops it in a random nest.
- A fraction of the nests containing the best eggs, or solutions, will carry over to the next generation.
- The number of nests is fixed and there is a probability that a host can discover an alien egg. If this happens, the host can discard the egg or the nest.

In CS optimisation, when generating a new solution X_i , it makes use of a Levy flight model

$$X_i^{(t+1)} = X_i^{(t)} + \vartheta \oplus \text{Levy}(\beta), \quad (11)$$

where ϑ is the step size related to the problem scale and is 1 in most cases, and \oplus means entry-wise multiplication. Various studies have shown that the flight behavior of many animals and insects has typical characteristics of Levy flights [24] which essentially model a random walk with random steps drawn from a Levy distribution for large steps

$$\text{Levy} \sim u = t^{-\lambda}, (1 < \lambda \leq 3), \quad (12)$$

which has an infinite variance with an infinite mean. Here, the consecutive jumps/steps of a cuckoo essentially form a random

Initialise a population of n host nests at random

while stopping criteria not met **do**

 Obtain a cuckoo X_i at random by Levy flights

 Choose a nest X_j randomly

if $F(X_i)$ better than $F(X_j)$ **then**

 Replace j by the new solution

end

 Abandon a fraction of the worse nests and create new ones using Levy flights

end

Algorithm 1: Cuckoo search (CS) algorithm

walk process which obeys a power-law step-length distribution with a heavy tail.

The CS is outlined in Algorithm 1.

E. CS-PFCM clustering

In our proposed approach, cuckoo search is used to find the optimal partitioning of the data given the possibilistic fuzzy c-means objective function. CS is initialised with random cluster centers. The cluster centers are then updated using the CS principles aiming to minimise the PFCM function. The stopping criterion is either the cluster centers having converged or having reaching a maximum number of iterations.

F. Pre- and post-processing

Before segmentation, the image is pre-processed to obtain a brightness corrected image to facilitate subsequent segmentation. For this, we simply calculate the global mean of the brightness $gMean$ over the whole image and pass over the image in a window of large size to ensure that the mean brightness inside the window $wMean$ is proportional to the global mean $gMean$. The new brightness value for the center pixel of the window is calculated as

$$\text{Pixel Brightness} = \frac{\text{Pixel Brightness}}{wMean} * gMean. \quad (13)$$

In a post-processing stage, we aim to remove small individual connected components, close small gaps and remove connected components with small thinness ratios. To remove small connected components and fill small gaps we make use of a rank order filter with size 3×3 and rank 5.

IV. EXPERIMENTAL RESULTS

A. Datasets

In our experiments, we have used two widely employed benchmark datasets, the DRIVE [14] and the STARE [25] databases, in order to assess the performance of our proposed algorithm.

The DRIVE database consists of a total of 40 colour fundus photographs of which 7 are abnormal pathology cases showing exudates, hemorrhages and pigment epithelium changes. Each image is JPEG compressed, which is common practice in screening programs, and has a resolution of 584×565 pixels with 8 bits per colour channel. The set of 40 images is divided into a training set of 20 images and test set comprising the

remaining 20. For the training set, for each image one manual segmentation, obtained from an ophthalmological expert, is provide, while for the test set, for each image two manual segmentations by two different observers are given, where the first observer segmentation is accepted as the ground-truth for performance evaluation.

The STARE database consists of a total of 20 eye fundus colour images where 10 contain pathologies. Each image has a resolution of 700×605 pixels with eight bits per color channel and is stored in PPM format.

B. Performance measures

For evaluation purposes, we employ the usual performance measures of sensitivity (Se), specificity (Sp) and accuracy (Acc), defined as

$$Se = TP / (TP + FN), \tag{14}$$

$$Sp = TN / (TN + FP), \tag{15}$$

and

$$Acc = (TP + TN) / (TP + FN + TN + FP), \tag{16}$$

where the true positives (TP) are correctly identified vessel pixels, false negatives (FN) are vessel pixels incorrectly classified as non-vessel, true negatives (TN) are correctly identified background pixels, and false positives (FP) are background pixels incorrectly classified as vessel pixels. The measures are computed individually for each image and then averaged over the whole test image set.

C. Results and discussion

Table I shows the performance of our proposed algorithm on the DRIVE dataset. Cuckoo search is optimised with 100 iterations and the population size was set to 20. The results confirm the robustness of our algorithm against changes in the input image and stable accuracy regardless of whether the input image is normal or abnormal since it gives roughly the same result even for images that contain exudates, hemorrhages and

TABLE I: Segmentation performance on the DRIVE database.

image	sensitivity	specificity	accuracy
1	0.739	0.977	0.945
2	0.630	0.993	0.937
3	0.630	0.978	0.927
4	0.477	0.996	0.926
5	0.611	0.990	0.938
6	0.618	0.984	0.932
7	0.528	0.994	0.931
8	0.673	0.944	0.909
9	0.577	0.989	0.940
10	0.617	0.988	0.943
11	0.511	0.995	0.931
12	0.691	0.978	0.941
13	0.539	0.993	0.927
14	0.702	0.974	0.942
15	0.694	0.977	0.947
16	0.557	0.993	0.935
17	0.653	0.982	0.941
18	0.688	0.984	0.949
19	0.756	0.989	0.960
20	0.740	0.977	0.951
average	0.628	0.984	0.938

TABLE II: Segmentation performance on the STARE database.

image	sensitivity	specificity	accuracy
1	0.618	0.962	0.924
2	0.617	0.971	0.938
3	0.755	0.958	0.941
4	0.491	0.990	0.938
5	0.437	0.979	0.911
6	0.676	0.979	0.952
7	0.644	0.996	0.957
8	0.617	0.997	0.957
9	0.631	0.996	0.956
10	0.645	0.970	0.934
11	0.585	0.996	0.956
12	0.676	0.996	0.961
13	0.628	0.993	0.948
14	0.606	0.994	0.945
15	0.645	0.990	0.948
16	0.509	0.993	0.924
17	0.545	0.997	0.941
18	0.418	0.999	0.958
19	0.392	0.996	0.96
20	0.512	0.989	0.945
average	0.586	0.987	0.94478

pigment epithelium changes. Even better results can be noted for the STARE images whose results are given in Table II.

Figure 1 on the left shows a sample image from the DRIVE dataset where we can notice brightness changes across the image. On the right of the figure is the corrected image after the pre-processing phase. It is apparent, that after pre-processing the image brightness is much more homogeneous over the image while maintaining the contrast between vessels and the background.

Figure 2 displays an example of the resulting segmented image using the CS-PFCM algorithm and the applied post-processing operations. As can be seen, the blood vessels appear clearly segmented in the final image.

V. CONCLUSIONS

In this paper, we have proposed a novel algorithm for segmenting blood vessels in retina images. Our approach makes use of the objective function for possibilistic fuzzy c-means clustering which is optimised using a cuckoo search technique which searches the clustering space successfully to minimise the PFCM objective function. Experimental evaluation proves our approach to be accurate and robust against

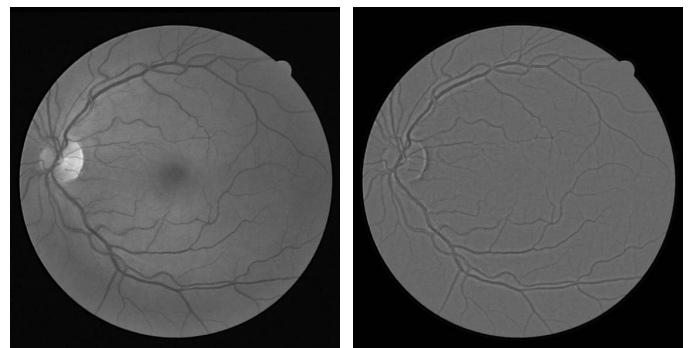


Fig. 1: Sample image from the DRIVE database (left) and the pre-processed image (right)

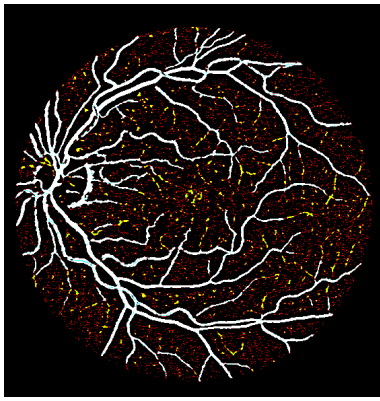


Fig. 2: Example image after segmentation and post-processing. Red pixels are removed by the rank order filter, yellow pixels are removed using a thinness measure and cyan pixels are pixels filled after closing.

noise and pathologies such as exudates, hemorrhages and pigment epithelium changes, and to provide good segmentation performance.

REFERENCES

- [1] M.M. Fraz, P. Remagnino, A. Hoppe, B. Uyyanonvara, A.R. Rudnicka, C.G. Owen and S.A. Barman, "Blood vessel segmentation methodologies in retinal images-a survey", *Comput. Methods Programs Biomed.*, Vol. 108, No. , pp. 407-433, 2012.
- [2] J.J. Wang, B. Taylor, T.Y. Wong, B. Chua, E. Rochtchina, R. Klein and P. Mitchell, "Retinal vessel diameters and obesity: a population-based study in older persons", *Obesity (Silver Spring)*, Vol. 14, No. 2, pp. 206-14, 2006.
- [3] M. Foracchia, E. Grisan and A. Ruggeri, "Extraction and quantitative description of vessel features in hypertensive retinopathy fundus images", 2nd international workshop on computer assisted fundus image analysis, 2011.
- [4] P. Mitchell, H. Leung, J.J. Wang, E. Rochtchina, A.J. Lee, T.Y. Wong and R. Klein, "Retinal vessel diameter and open-angle glaucoma: the blue mountains eye study", *Ophthalmology*, Vol. 112, No. 2, pp. 245-250, 2005.
- [5] K. Goatman, A. Charnley, L. Webster and S. Nussey, "Assessment of automated disease detection in diabetic retinopathy screening using two-field photography", *PLoS. One*, Vol. 6, No.12, pp. 275-284, 2011.
- [6] C. Heneghan, J. Flynn, M. OKeefe and M. Cahill, "Characterization of changes in blood vessel width and tortuosity in retinopathy of prematurity using image analysis", *Med. Image Anal.* vol. 6, pp. 407-429, 2002.
- [7] J. Lowell, A. Hunter, D. Steel, A. Basu, R. Ryder, R.L.Kennedy, "Measurement of retinal vessel widths from fundus images based on 2D modeling", *IEEE Trans. Med. Imaging*, Vol. 23, pp. 1196-1204, 2004.
- [8] A. Haddouche, M. Adel, M. Rasigni, J. Conrath and S. Bourenane, "Detection of the foveal avascular zone on retinal angiograms using markov random fields:", *Digital Signal Processing*, Vol. 20, pp. 149-154, 2010.
- [9] E. Grisan and A. Ruggeri, "A divide et impera strategy for automatic classification of retinal vessels into arteries and veins", in *Engineering in medicine and biology society, Proc of the 25th annual international conf. of the IEEE*, Vol. 891, pp. 890-893, 2003.
- [10] J.J. Kanski, "Clinical Ophthalmology", 6th ed., Elsevier Health Sciences, London, UK, 2007.
- [11] C. Klse and C. Ikibas, "A personal identification system using retinal vasculature in retinal fundus images", *Expert Systems with Applications*, vol. 38, pp. 13670-13681, 2011.
- [12] V. Vijayakumari and N. Suriyanarayanan, "Survey on the detection methods of blood vessel in retinal images", *Eur. J. Sci. Res.*, Vol. 68, No.1, pp. 83-92, 2012.
- [13] X. You, Q. Peng, Y. Yuan, Y. Cheung and J. Lei, "Segmentation of retinal blood vessels using the radial projection and semi-supervised approach", *Pattern Recogn.*, Vol. 441, pp. 2314-2324, 2011.
- [14] J.J. Staal, M.D. Abramoff, M. Niemeijer, M.A. Viergever and B. van Ginneken, "Ridge based vessel segmentation in color images of the retina", *IEEE Trans. Med. Imaging*, Vol. 23, No. 4, pp. 501-509, 2004.
- [15] D. Marin, A. Aquino, ME. Gegundez-Arias and JM. Bravo, "A new supervised method for blood vessel segmentation in retinal images by using grey-level and moment invariants-based features", *IEEE Trans. Med. Imaging*, Vol. 30, No. 1, pp. 146-158, 2011.
- [16] M. M. Fraz, S. A. Barman, P. Remagnino, A. Hoppe, A.Basit, B. Uyyanonvara, A. R. Rudnicka, and C.G. Owen, "An ensemble classification-based approach applied to retinal blood vessel segmentation", *IEEE Trans. Biomed. Eng.*, Vol. 59, No. 9, pp. 1427-1435, 012.
- [17] M. S. Miri and A. Mahloojifar, "Retinal image analysis using curvelet transform and multistructure elements morphology by reconstruction", *IEEE Trans. Biomed. Eng.*, Vol. 58, No. 5, pp. 1183-1192, 2011.
- [18] M. M. Fraz, S. A. Barman, P. Remagnino, A. Hoppe, A.Basit, B. Uyyanonvara, A. R. Rudnicka, and C.G. Owen, "An approach to localize the retinal blood vessels using bit planes and centerline detection", *Comput. Methods Programs Biomed.*, 2011.
- [19] K.K. Delibasis, A.I. Kechriniotis, C. Tsonos and N. Assimakis, "Automatic model-based tracing algorithm for vessel segmentation and diameter estimation", *Comput. Method. Programs. Biomed.*, Vol. 100, pp. 108-122, 2010.
- [20] B. Zhang, L. Zhang, L. Zhangb and F. Karray, "Retinal vessel extraction by matched filter with first-order derivative of Gaussian", *Comput. Biol. Med.*, Vol. 40 , pp. 438-445, 2010.
- [21] N. R. Pal , K. Pal , J. M. Keller and J. C. Bezdek "A possibilistic fuzzy c-means clustering algorithm", *IEEE Trans. Fuzzy Syst.*, Vol. 13, pp. 517-530, 2005
- [22] Raghuram Krishnapuram, James M. Keller: A possibilistic approach to clustering. *IEEE T. Fuzzy Systems*, Vol. 1, No. 2.
- [23] Yang, X.S. and S. Deb, 2009. Cuckoo search via Levy flight. *Proceeding of World Congress on Nature and Biologically Inspired Computing*, pp. 210-214, 2009.
- [24] Brown, C., Liebovitch, L. S., Glendon, R., "Levy flights in Dobe Ju'hoansi foraging patterns", *Human Ecol.*, Vol. 35, No. 1, pp. 129-138, 2007.
- [25] A. Hoover, V. Kouznetsova, and M. Goldbaum, "Locating blood vessels in retinal images by piecewise threshold probing of a matched filter response," *IEEE Trans. Med. Imag.*, vol. 19, no. 3, pp. 203-211, 2000.